Published for SISSA by Springer

Received: *September 15, 2015*
Accepted: *October 12, 2015*
Published: *November 17, 2015*

Segmented strings in AdS_3

Nele Callebaut,[a] Steven S. Gubser,[a] Andreas Samberg[b,c] and Chiara Toldo[d]

[a] *Joseph Henry Laboratories, Princeton University, Princeton, NJ 08544, U.S.A.*

[b] *Institut für Theoretische Physik, Ruprecht-Karls-Universität Heidelberg, Philosophenweg 16, 69120 Heidelberg, Germany*

[c] *ExtreMe Matter Institute EMMI, GSI Helmholtzzentrum für Schwerionenforschung, Planckstraße 1, 64291 Darmstadt, Germany*

[d] *Department of Physics, Columbia University, 538 West 120th Street, New York, NY 10027, U.S.A.*

E-mail: ct2673@columbia.edu, ssgubser@princeton.edu, a.samberg@thphys.uni-heidelberg.de, nmc2159@columbia.edu

Abstract: We study segmented strings in flat space and in AdS_3. In flat space, these well known classical motions describe strings which at any instant of time are piecewise linear. In AdS_3, the worldsheet is composed of faces each of which is a region bounded by null geodesics in an AdS_2 subspace of AdS_3. The time evolution can be described by specifying the null geodesic motion of kinks in the string at which two segments are joined. The outcome of collisions of kinks on the worldsheet can be worked out essentially using considerations of causality. We study several examples of closed segmented strings in AdS_3 and find an unexpected quasi-periodic behavior. We also work out a WKB analysis of quantum states of yo-yo strings in AdS_5 and find a logarithmic term reminiscent of the logarithmic twist of string states on the leading Regge trajectory.

Keywords: Bosonic Strings, AdS-CFT Correspondence

ArXiv ePrint: 1508.07311

doi:10.1007/JHEP11(2015)110

Contents

1 Introduction

Strings in flat space are simple because their dynamics is controlled by a free conformal field theory (CFT). Strings in general curved spacetimes are relatively intractable because, even if the constraint of conformal invariance is obeyed, the worldsheet CFT is too complicated to solve. Strings in anti-de Sitter (AdS) space are a happy medium, where the worldsheet CFT is interacting but is understood to be integrable. For entry points into the large literature on integrability, see for example [1, 2]. Classical string solutions in AdS have been treated systematically when their motion is a rigid rotation: as reviewed in [2], one can then map the problem of finding their shape into an integrable one-dimensional Neumann model describing some variant of an oscillator on a sphere. This method, together with some extensions, allows for the construction of quite a variety of string states. Other methods, including Pohlmeyer reduction, Bäcklund transformations, coset methods, and the dressing method, have been used to produce an extensive and varied collection of classical solutions: see for example [3–13].

In this paper we focus on a class of classical string motions in AdS_3 which can be analyzed by elementary means. The string configurations can be thought of as segmented, where each segment stretches along the intersection of a time-slice in AdS_3 with an AdS_2 subspace. Tracking the motion of the string is as simple as tracking the lightlike motion of the points where the segments join together. An analogous class of classical string motions in flat space has been studied extensively starting with [14] and is central to the Lund model of mesons [15]. In the Lund model, a basic ingredient is the yo-yo string, where a string starts at rest stretched between two points, and then contracts inward until its endpoints meet. Then it expands outward again until it regains its original length, and contracts once again. An interesting point is that any piecewise linear string can be constructed as a union of boosted yo-yos, joined up so that one endpoint matches with the next. There is a small caveat: generically, we may expect that a string solution does not have finite momentum localized at a point, but yo-yos do, except when they reach their full length. We will adopt a simple treatment where we think of dropping the endpoint momentum when two yo-yo solutions are joined at their endpoints.[1] Yo-yo strings were studied in AdS_5 in [16]. For earlier related work see [17, 18]; in the latter work [18], segmented strings were considered on an $\mathbf{R} \times S^5$ subspace of $AdS_5 \times S^5$.

A variant of the yo-yo is possible in AdS_3, where a string undergoes yo-yo motions while its center of mass stays fixed at the center of AdS_3. Just as we can boost a yo-yo solution in flat space, we can apply a (global) conformal transformation to a yo-yo solution in AdS_3. Even after an arbitrary global conformal transformation, the yo-yo will move in some AdS_2 subspace of AdS_3. We can assemble conformally transformed yo-yos in the same way as in flat space, dropping endpoint momentum where yo-yo endpoints join together. In this way we obtain the classical closed string motions we are interested in. Treating open string motions similarly requires inclusion of localized momentum and is beyond our current scope.

The discussion of the previous two paragraphs leaves out an important aspect of time evolution. If we are considering segmented strings with kinks where segments join, then as the string propagates forward in time, we have to ask what happens when kinks collide. The answer, it turns out, can be worked out almost completely from considerations of causality. As a warm-up, in section 2 we will explain how segmented strings work in flat space. The results are trivial in the sense that we are only recovering the results of free field theory. The main results are in section 3, where we explain the evolution of segmented strings in AdS_3 as well as a partial account of initial conditions. Section 4 is devoted to energy considerations, including computation of the conserved energy of strings in AdS_3 and a WKB analysis of energy levels. In section 5 we present some examples of motions of segmented strings in AdS_3 which are non-periodic.

[1]This approach imposes some limits on the class of string solutions we are able to study. For example, we cannot in this way study a string doubled over on itself, because as the doubled-over part contracts, finite momentum collects at the kink.

JHEP11(2015)110

2 Piecewise linear strings

Classical trajectories of closed strings in flat space must take the form

$$X^\mu(\tau,\sigma) = \frac{1}{2}\left(Y_R^\mu(\tau-\sigma) + Y_L^\mu(\tau+\sigma)\right) . \tag{2.1}$$

As written, eq. (2.1) is the general solution to the flat space string equations of motion written in conformal gauge. The Virasoro constraints are satisfied if $Y_R^\mu(\xi)$ and $Y_L^\mu(\xi)$ are null trajectories in spacetime. Any such trajectory can be approximated by a piecewise linear null trajectory. If we do this for Y_R^μ and Y_L^μ, then the $X^\mu(\tau,\sigma)$ are piecewise linear functions of τ and σ. Such string motions are precisely the segmented strings we are interested in.

On any time slice (meaning a slice of constant X^0), a segmented string must be a union of line segments, each of whose center of mass follows a timelike trajectory while its endpoints move at the speed of light. The endpoints are kinks where the direction of spatial extent of the string along a fixed timeslice can change. Thus we see that segmented strings can indeed be regarded as a union of boosted yo-yo solutions, except without endpoint momentum. The time evolution of the string can easily be described by tracking the kinks until two kinks collide. As we will explain, we can determine the "outcome" of such a collision, namely the direction of two new kinks that come out of the collision, based on knowing only the geometry of the string worldsheet in a small neighborhood of the collision. In other words, to know the entire motion of a piecewise linear string, one has only to track the motion and interactions of finitely many piecewise null geodesics on its worldsheet, using only local information at the kinks.

The conclusions of the previous paragraph are trivial in the sense that we are only restructuring the solution eq. (2.1). But it is an appealing thought that the description of string dynamics that we will give generalizes to the far less trivial problem of strings in curved spacetime. In short, we make the following conjectures:

- There are classical string trajectories in suitable curved spacetimes which can be completely described by tracking the piecewise null trajectories of finitely many points on the string worldsheet, together with the direction of the string worldsheet running into and out of each of these points.

- The space of all the trajectories capable of such description is dense in the space of all possible classical string motions.

By "suitable curved spacetimes" we mean spacetimes in which strings can consistently propagate — which in terms of conformal field theory means target spaces whose beta functionals vanish.

Before exploring these conjectures further, let's articulate in flat space exactly how a description of classical string motion works when we specify data only in the vicinity of several lightlike kinks. Let these kinks be numbered $i = 1, 2, \ldots, N$, and let their spatial positions be

$$\vec{x}_i(t) = \vec{v}_i t + \vec{d}_i \, . \tag{2.2}$$

(Of course, the linear form eq. (2.2) of $\vec{x}_i(t)$ only applies piecewise: that is, $\vec{v}_i$ and $\vec{d}_i$ change discontinuously at special times when kinks collide.) Assume further that the string (which we take to be oriented) runs into kink i along a spatial unit vector $\vec{\ell}_i$, and out of it along a spatial unit vector $\vec{r}_i$. We can uniquely decompose

$$\vec{v}_i = v_{iL}\vec{\ell}_i + \vec{v}_{iT} = v_{iR}\vec{r}_i + \vec{v}_{iS} \tag{2.3}$$

where $\vec{v}_{iT} \perp \vec{\ell}_i$ and $\vec{v}_{iS} \perp \vec{r}_i$. The velocity $\vec{v}_{iT}$ ($\vec{v}_{iS}$) is the transverse velocity of the string running into (out of) the kink, and because this velocity must be timelike, the signed real quantity v_{iL} (v_{iR}) must be non-zero. We make an important restriction on the states we allow by requiring the product $v_{iL}v_{iR}$ to be positive. Physically, the kink must either be moving to the right along the string, in which case $v_{iR} > 0$, or left along the string, in which case $v_{iR} < 0$. If we considered cases where $v_{iL}v_{iR} < 0$, then we have to allow finite momentum at the kink, whose linear increase or decrease with time would be part of the dynamics.

An additional constraint is that the string running out of kink i must connect with the string running into kink $i+1$: that is, $\vec{r}_i = \vec{\ell}_{i+1}$ must be the unit vector in the direction of $\vec{x}_{i+1}(t) - \vec{x}_i(t)$. There are now three subcases to consider:

- If kink i is right-moving while kink $i+1$ is left-moving, then the two kinks will collide at some future time t_*, and one can see that $\vec{r}_i = \vec{\ell}_{i+1}$ is the unit vector parallel to $\vec{v}_i - \vec{v}_{i+1}$.
- If kink i is left-moving while kink $i+1$ is right-moving, then the two kinks came out of a collision at some earlier time t_*, and $\vec{r}_i = \vec{\ell}_{i+1}$ is the unit vector parallel to $\vec{v}_{i+1} - \vec{v}_i$.
- If both kinks are right-moving, or both are left-moving, then $\vec{v}_i = \vec{v}_{i+1}$, and $\vec{r}_i = \vec{\ell}_{i+1}$ is the unit vector parallel to $\vec{d}_{i+1} - \vec{d}_i$.

Here and below, what we mean by two vectors $\vec{a}$ and $\vec{b}$ being parallel is that $\vec{a} = \lambda\vec{b}$ for some positive real number λ. If instead λ were negative, we would refer to $\vec{a}$ and $\vec{b}$ as anti-parallel.

Thus far, we have only described the time evolution of kinks in the absence of collisions between kinks, along with consistency conditions that must be satisfied throughout that time evolution. To describe a collision, first note that we must start with a right-moving kink to the left of a left-moving kink and end up instead with a left-moving kink to the left of a right-moving kink. The key point in predicting the outcome of a collision of kinks is that the spatial orientation and transverse motion of the string running into the leftmost kink cannot change: that is, $\vec{\ell}_i$ and $\vec{v}_{iT}$ are unaltered by the collision. This conclusion can be reached on grounds of causality applied to the string segment running into the leftmost kink. Whatever happens at the collision, a piece of string at some finite distance away from the collision cannot find out about it until the newly formed kink traverses back across the string at the speed of light. By a similar argument, $\vec{r}_{i+1}$ and $\vec{v}_{i+1,S}$ are unaltered. What does happen at the collision is that kinks pass through one another, or bounce off each other, and the leftmost one starts moving back along the worldsheet (i.e. to the left) while the rightmost one moves forward along the worldsheet (i.e. to the right). The only way this can happen is if the kink's longitudinal velocities after the collision are given by

$$\tilde{v}_{iL} = -v_{iL} \qquad\qquad \tilde{v}_{i+1,R} = -v_{i+1,R} \tag{2.4}$$

By demanding that $\vec{x}_i(t)$ and $\vec{x}_{i+1}(t)$ are continuous at the time $t = t_*$ of the collision, we straightforwardly obtain the relations

$$\tilde{\vec{d}}_i = \vec{d}_i + 2v_{iL}\vec{\ell}_i t_* \qquad\qquad \tilde{\vec{d}}_{i+1} = \vec{d}_{i+1} + 2v_{i+1,R}\vec{r}_{i+1}t_* \,. \tag{2.5}$$

Finally, we should ask in what spatial direction the string between the kinks runs along after the collision. The answer is that this direction, $\vec{r}_i = \vec{\ell}_{i+1}$, is the unit vector parallel to $\tilde{\vec{v}}_{i+1} - \tilde{\vec{v}}_i$.

In summary: equations (2.2)–(2.5) are sufficient to determine the motion of piecewise linear strings assuming that there is no localized energy or momentum at the kinks between linear segments. We could regard the case where there is localized energy or momentum at a kink as a limit of a situation where a very short segment of string propagates at nearly the speed of light.

3 Strings in AdS_3

Let us now consider strings in AdS_3, which we describe as the locus of points in $\mathbf{R}^{2,2}$ satisfying the equation

$$-(Y^{-1})^2 - (Y^0)^2 + (Y^1)^2 + (Y^2)^2 = -1 \,. \tag{3.1}$$

We may parametrize the locus with coordinates (τ, ρ, ϕ) as

$$\begin{pmatrix} Y^{-1} \\ Y^0 \\ Y^1 \\ Y^2 \end{pmatrix} = \begin{pmatrix} \cosh\rho\cos\tau \\ \cosh\rho\sin\tau \\ \sinh\rho\cos\phi \\ \sinh\rho\sin\phi \end{pmatrix} . \tag{3.2}$$

AdS_3 is in fact the universal covering space of the hyperboloid eq. (3.1); in practical terms this means that as global time τ evolves forward by 2π, we do not return to the same point, but instead to a new sheet of the covering space.

3.1 The yo-yo in AdS_3

As in the introduction, we will start our discussion of string motions in AdS_3 with the yo-yo. Assume that at time $\tau = 0$, the string starts at $\rho = 0$, and after some time it expands to stretch from $(\rho, \phi) = (\rho_*, \pi)$ to $(\rho, \phi) = (\rho_*, 0)$. This string lies wholly in the AdS_2 submanifold specified by intersecting the hyperboloid eq. (3.1) with the plane $Y_2 = 0$. We rewrite the equation $Y_2 = 0$ as

$$k_A Y^A = 0 \tag{3.3}$$

where $k^A = (0,0,0,1)$ and we raise indices with the natural metric diag$\{-1,-1,1,1\}$ on $\mathbf{R}^{2,2}$. The right-moving endpoint of the yo-yo travels along the null geodesic

$$Y^A(\xi) = h^A + v^A \xi \tag{3.4}$$

where $h^A = (1,0,0,0)$ and $v^A = (0, 1/\sqrt{2}, 1/\sqrt{2}, 0)$. (An important observation is that eq. (3.4) is a null geodesic both in the embedding spacetime $\mathbf{R}^{2,2}$ and on the hyperboloid AdS_3 defined by eq. (3.1).) Observe that h, k, and v are mutually orthogonal, and if we include also $u^A = (0, 1/\sqrt{2}, -1/\sqrt{2}, 0)$ we have a basis

$$B = (h, k, u, v) \tag{3.5}$$

which satisfies the relations

$$\begin{array}{llll} h^2 = -1 & k^2 = 1 & u^2 = 0 & v^2 = 0 \\ h \cdot k = h \cdot u = h \cdot v = 0 & k \cdot u = k \cdot v = 0 & u \cdot v = -1\,. & \end{array} \tag{3.6}$$

An overall multiplicative factor on v can be adjusted at will, provided we correspondingly rescale u to maintain the relation $u \cdot v = -1$. Define now t as the unit vector field on AdS_3 in the direction of $d/d\tau$. We require that $t \cdot v$ and $t \cdot u$ are negative; that is, v and u are future-directed. If it is desired to fix the freedom of adjusting v by an overall multiplicative factor, we may additionally demand $t \cdot v = -1/\sqrt{2}$. Note that in general it is not consistent to demand additionally $t \cdot u = -1/\sqrt{2}$.

Observe for the basis indicated below eq. (3.4) that

$$v^A = -\epsilon^A{}_{BCD} h^B k^C v^D \tag{3.7}$$

where ϵ_{ABCD} is antisymmetric with $\epsilon_{-1,0,1,2} = 1$. If instead we started with $v^A = (0, 1/\sqrt{2}, -1/\sqrt{2}, 0)$, with $k^A = (0,0,0,1)$ and $h^A = (1,0,0,0)$ as before, then to satisfy eq. (3.6) we would need $u^A = (0, 1/\sqrt{2}, 1/\sqrt{2}, 0)$, which results in a coordinate system with the opposite orientation: that is, the explicit minus sign would be absent on the right hand side of eq. (3.7). We will refer to a basis B satisfying eq. (3.7) as having orientation $\sigma(B) = +1$, while if the explicit minus were absent, we would say $\sigma(B) = -1$.

In summary, the right-moving kink at the tip of yo-yo can be characterized by a basis B_L with orientation $+1$, while the left-moving kink can be characterized by a basis B_R of orientation -1; and the bases B_L and B_R share the same vectors h and k, while the forward-directed null vectors u and v are flipped between B_L and B_R, up to possible rescalings of v (and hence u) which correspond to rescalings of ξ_L and ξ_R. The choice of the spacelike vector k specifies the AdS_2 subspace in which the yo-yo propagates; the timelike vector h specifies the moment at which the two ends of the yo-yo begin to separate; and of course the vectors v_L and v_R indicate the null directions within AdS_2 in which the right-moving and left-moving kinks propagate.

It is easy enough to predict how the yo-yo will evolve because it remains always in the same AdS_2 subspace. Namely, the endpoints start off with some definite momentum, which for simplicity we assume to be equal and opposite. (More technically, the sum of the energy-momentum vectors of the two endpoints at the initial point h where they coincide is in the direction of t; if this is not the case we can change t by a conformal transformation to make it so, amounting to some $\mathrm{SO}(2,2)$ transformation on $\mathbf{R}^{2,2}$.) The energy and momentum bleed off from the endpoint into the bulk of string as it extends in the spatial direction of AdS_2 until no energy remains; then the endpoints snap back and propagate along null trajectories back to a position in AdS_2 which is h plus some positive multiple of t.

It will pay to give a slightly more explicit description of this motion in terms of the bases B_L and B_R. For either basis (dropping the subscript for notational simplicity), the evolution with affine parameter ξ along a null trajectory is given by

$$h(\xi) = h + \xi v \qquad k(\xi) = k \qquad u(\xi) = u - \xi h - \frac{\xi^2}{2} v \qquad v(\xi) = v \,, \tag{3.8}$$

where h, k, u, and v on the right hand sides are understood to be the initial values at $\xi = 0$. The evolution $h(\xi)$ is what we mean by advancing along a null trajectory. Keeping k and v constant simply means that we stay on a definite null trajectory within a definite AdS_2 subspace. The form of $u(\xi)$ is forced upon us by the requirement of preserving the orthogonality relations eq. (3.6). Alternatively, we may arrive at this evolution by parallel transporting u along the null trajectory, using the natural connection on AdS_3 (not the trivial connection on $\mathbf{R}^{2,2}$). Note that the condition $t \cdot v = -1/\sqrt{2}$ is not preserved by the evolution eq. (3.8): a direct calculation of t along the null geodesic yields

$$t(\xi) = \frac{u + v - \xi h}{\sqrt{2 + \xi^2}} \,, \tag{3.9}$$

so $t(\xi) \cdot v(\xi) = -1/\sqrt{2 + \xi^2}$.

Snap-back occurs at some value $\xi = \xi_*$ which depends on the initial energy and momentum carried by the endpoints. Snap-back is easy to describe in terms of basis vectors: one simply swaps v and u, keeping h and k the same. As a result, the orientation of each basis flips. We may then reapply the time evolution eq. (3.8) to each new basis, with the result that the endpoints travel back toward one another as summarized previously. When they meet, they should be understood to pass through one another, separating once more to the same maximum distance before snapping back again.

3.2 Closed strings in AdS_3

The generalization of the yo-yo that we propose is the closest analog to piecewise linear strings that can be achieved in AdS_3. Namely, on a particular slice of constant global time τ, let there be N kinks, which are cyclically arranged in the order in which the string passes through them. The string is, by assumption, oriented and closed, so we think of the string as starting at kink $i = 1$, proceeding to $i = 2$, and so on up to kink $i = N$, and finally back to kink $i = 1$. For simplicity, we stipulate as before that there is no localized energy or momentum at the kinks. Each kink is "decorated" with an "extended basis," call it B_i, which comprises *six* vectors in $\mathbf{R}^{2,2}$: dropping the index i for simplicity,

$$B = (h, j, k, w, u, v) \,. \tag{3.10}$$

In addition to the relations eq. (3.6), we demand also

$$\begin{aligned} &j^2 = 1 && w^2 = 0 && \\ &h \cdot j = h \cdot w = 0 && j \cdot w = j \cdot v = 0 && w \cdot v = -1\,. \end{aligned} \tag{3.11}$$

In short, (h, k, u, v) is a basis in the sense of eq. (3.6), characterizing the string running out from the kink, and (h, j, w, v) is another such basis characterizing the string running into the kink. We also require that these two bases have the same orientation in the sense explained following eq. (3.7) (with w future-directed like v and u are); we will refer to this orientation as $\sigma(B) = \pm 1$. Explicitly, if eq. (3.7) holds as written, then we must also have

$$v^A = -\epsilon^A{}_{BCD} h^B j^C v^D\,. \tag{3.12}$$

If $\sigma(B) = +1$, then the corresponding kink is right-moving in the sense that the string segment running into it (i.e. from the left in worldsheet terms) is lengthening with increasing global time τ, while the string segment running out of it (i.e. to the right in worldsheet terms) is shortening. If $\sigma(B) = -1$, then the kink is left-moving on the worldsheet.

Time evolution of the string worldsheet is a generalization of the discussion of the yo-yo. The formula (3.8) may be augmented by the rules

$$j(\xi) = j \qquad w(\xi) = w - \xi h - \frac{\xi^2}{2} v \tag{3.13}$$

and applied to each basis. We must arrange initial conditions so that adjacent kinks with opposite orientation collide either in the future or in the past, and so that the kinks' trajectories lie on a common AdS_2 subspace. Let's treat the case of a right-moving kink 1 and a left-moving kink 2; then the collision must happen in the future. We first use eq. (3.8) and eq. (3.13) to advance the kinks to the collision point. For simplicity we now drop all reference to ξ and simply assume that the extended bases $B_1 = (h_1, j_1, k_1, w_1, u_1, v_1)$ and $B_2 = (h_2, j_2, k_2, w_2, u_2, v_2)$ satisfy

$$h_1 = h_2 \qquad k_1 = j_2\,. \tag{3.14}$$

To work through the logic of a collision, it helps to consider first the "outer" segments of string, namely the string segment running into kink 1 and the segment running out of kink 2. These segments must remain in the same spatial orientation — that is, j_1 and k_2 are unchanged. The reason is that if we go out a little way along either of the outer segment, then we are spacelike separated from the collision itself, and nothing about the collision can affect the motion of the string where we are. Of course, h_1 and h_2 are also unchanged. Let's improve notation and write

$$\tilde{h}_1 = \tilde{h}_2 = h_1 = h_2 \qquad \tilde{j}_1 = j_1 \qquad \tilde{k}_2 = k_2\,, \tag{3.15}$$

where a tilde is used to indicate data relating to after the collision. We may further reason that

$$\tilde{v}_1 = w_1 \qquad \tilde{w}_1 = v_1 \qquad \tilde{v}_2 = u_2 \qquad \tilde{u}_2 = v_2\,. \tag{3.16}$$

JHEP11(2015)110

The justification for $\tilde{v}_1 = w_1$ is that after the collision, it must travel in a forward-directed null direction within the AdS_2 subspace orthogonal to j_1, and the only such direction other than v_1 is w_1. Then we must have $\tilde{w}_1 = v_1$ to maintain orthogonality relations. The third and fourth equations of eq. (3.16) can be justified similarly. This reasoning is perfectly analogous to the description of snap-back for the yo-yo. Note that due to swapping v_1 and w_1, now kink 1 has orientation -1 (that is, it is left-moving), while kink 2 has flipped its orientation to $+1$, i.e. right-moving. Thus we preserve the order of the kinks through the collision; intuitively, we think of the kinks as bouncing back off one another rather than passing through one another.

In order to figure out what happens to the "inner" segment of string after the collision, let's first note that we know $\tilde{v}_1$ and $\tilde{v}_2$ from eq. (3.16). These two null vectors at the collision point uniquely determine the AdS_2 subspace in which the inner segment of string must lie. Because $\tilde{v}_1$ and $\tilde{v}_2$ form a null basis for the tangent space of this AdS_2 subspace at the collision point, it must be that $\tilde{u}_1$ is some multiple of $\tilde{v}_2$ and $\tilde{w}_2$ is some multiple of $\tilde{v}_1$; only then can $(\tilde{v}_1, \tilde{u}_1)$ and $(\tilde{v}_2, \tilde{w}_2)$ also be bases for the same AdS_2 subspace at the collision point. More specifically:

$$\tilde{u}_1 = -\frac{\tilde{v}_2}{\tilde{v}_1 \cdot \tilde{v}_2} \qquad \tilde{w}_2 = -\frac{\tilde{v}_1}{\tilde{v}_1 \cdot \tilde{v}_2}\,, \tag{3.17}$$

where the denominators enforce the relevant orthogonality relations. At this point, the only vectors left are $\tilde{k}_1$ and $\tilde{j}_2$. These vectors determine the AdS_2 subspace in which the inner string propagates after the collision. But we already know which AdS_2 we want: it is the one through the collision point whose tangent space has basis $(\tilde{v}_1, \tilde{u}_1)$, or equivalently $(\tilde{v}_2, \tilde{w}_2)$. It is straightforward to check that

$$\tilde{k}_1^A = \tilde{j}_2^A = -\epsilon^A{}_{BCD}\tilde{h}_1^B \tilde{u}_1^C \tilde{v}_1^D \tag{3.18}$$

is the unique choice that will satisfy the orthogonality relations as well as eq. (3.7) and eq. (3.12) for kink 2 (which is right-moving), and the same conditions without the explicit minus signs for kink 1 (which is left-moving).

In eq. (3.14) we stated the minimal set of preconditions on the bases B_1 and B_2 before the collision required in order for the discussion eqs. (3.15)–(3.18) to make sense. In fact, if we run the logic of the collision in reverse, we can deduce some additional preconditions relating to the inner segment of string before the collision:

$$u_1 = -\frac{v_2}{v_1 \cdot v_2} \qquad w_2 = -\frac{v_1}{v_1 \cdot v_2} \qquad k_1^A = j_2^A = -\epsilon^A{}_{BCD} h_1^B u_1^C v_1^D\,. \tag{3.19}$$

3.3 Initial conditions

We have laid out string evolution so far without specifying exactly what initial conditions one is supposed to evolve from, say on the time-slice $\tau = 0$. A quick way out is to allow precisely those initial conditions which, if evolved forward in time, lead to collisions where the preconditions eq. (3.14) and eq. (3.19) are satisfied for every pair of colliding vertices, and if evolved backward in time, lead to collisions where for any pair of colliding vertices, call them kinks 1 and 2, we have $\tilde{h}_1 = \tilde{h}_2$, $\tilde{k}_1 = \tilde{j}_2$, and eq. (3.17).[2] In practice, we would like a more constructive account of allowed initial conditions.

We do not have complete results, but we will offer here a construction of initial conditions based on the assumption that one single collision of kinks occurs at time $\tau = 0$. Let there be N kinks total, with N stipulated to be an even number, and let the two kinks undergoing a collision at $\tau = 0$ be kinks number $N-1$ and N. Specify first the desired positions $h_1, h_2, \ldots, h_{N-1}$, h_N at time $\tau = 0$, with $h_{N-1} = h_N$ by assumption. Note that each position may be expressed as

$$h_i = (h_i^{-1}, 0, \vec{h}_i) \qquad \text{where} \qquad h_i^{-1} = \sqrt{1 + \vec{h}_i^2}\,, \tag{3.20}$$

and we use the short-hand $\vec{X}$ to mean the spatial components (X^1, X^2) of any vector in $\mathbf{R}^{2,2}$. The positive sign in front of the square root in eq. (3.20) must be chosen because that is what corresponds to $\tau = 0$ (rather than $\tau = \pi$). Thus in eq. (3.20), the quantities that can be freely specified are $\vec{h}_1, \vec{h}_2, \ldots, \vec{h}_{N-1}$, for a total of $2(N-1)$ real free parameters, subject to the condition that adjacent kinks must be distinct — and that includes the constraint that $\vec{h}_{N-1} = \vec{h}_N$ differs from $\vec{h}_1$.

Next, specify the spatial components $\vec{v}_1$ of the velocity v_1. The condition $h_1 \cdot v_1 = 0$ allows us to compute

$$v_1^{-1} = \frac{\vec{h}_1 \cdot \vec{v}_1}{h_1^{-1}}\,, \tag{3.21}$$

where we used $\tau = 0$ to conclude $h_0 = 0$. The condition $v_1 \cdot v_1 = 0$ is now a quadratic equation for v_1^0 whose solution is

$$v_1^0 = \sqrt{\vec{v}_1^2 - (v_1^{-1})^2}\,. \tag{3.22}$$

The quantity inside the square root must be positive because of the Schwarz inequality applied to eq. (3.21) together with $h_1^{-1} = \sqrt{1 + \vec{h}_1^2}$. We must choose the positive sign on the square root in eq. (3.22) because we want v_1 to be future directed. Note that no consideration in this paragraphs restricts $\vec{v}_1$ in any way, except that it should be non-zero in order for v_1 as a whole to be non-zero. Thus $\vec{v}_1$ adds two more free real parameters to the initial conditions, for a total of $2N$. We will see as we go on with our construction that not all values of $\vec{v}_1$ are allowed.

The plan now is to figure out what v_2 must be, then v_3, and so forth up to v_{N-1}. To determine v_2, we impose the condition that kinks 1 and 2 must collide at some future time τ_1, with no other kinks colliding with either 1 or 2 in the interval $0 < \tau < \tau_1$. (The case where kinks 1 and 2 collide at some time in the past proceeds almost identically.) Then we must be able to solve the equations

$$h_1 + \xi_1 v_1 = h_2 + \zeta_2 v_2 \qquad v_2 \cdot v_2 = h_2 \cdot v_2 = 0\,. \tag{3.23}$$

[2] This set of constraints is sufficient provided we alternate right-moving and left-moving kinks. If there are, for example, several left-moving kinks in a row, then we have to put constraints going forward in time on the leftmost one, which undergoes a collision with the right-moving kink just to its left, and then constrain the next-to-leftmost left-moving kink in terms of the right-moving kink emerging from said collision.

Moreover, the affine times ξ_1 and ζ_2 that elapse before kinks collide must be positive. We are free to rescale v_2 by a positive factor; let us use this freedom to set $\zeta_2 = \xi_1$. Defining

$$\Delta h_i = h_{i+1} - h_i \qquad \text{for} \qquad 1 \le i < N\,, \tag{3.24}$$

one can easily check that the unique solution for $\xi_1 = \zeta_2$ and v_2 is

$$\xi_1 = \zeta_2 = \frac{(\Delta h_1)^2}{2\Delta h_1 \cdot v_1} \qquad v_2 = v_1 - 2\frac{\Delta h_1 \cdot v_1}{(\Delta h_1)^2}\Delta h_1\,. \tag{3.25}$$

Note that our assumption that h_1 and h_2 are distinct implies $(\Delta h_1)^2 > 0$, since this inequality is the statement that h_1 and h_2 are spacelike separated. So we must have $\Delta h_1 \cdot v_1 > 0$, which can be re-expressed as the constraint

$$h_2 \cdot v_1 > 0\,, \tag{3.26}$$

or, after the use of eq. (3.21),

$$\vec{v}_1 \cdot \left(\frac{\vec{h}_2}{h_2^{-1}} - \frac{\vec{h}_1}{h_1^{-1}} \right) > 0\,. \tag{3.27}$$

We next require that kinks 2 and 3 must have collided at some time τ_2 in the past, with no collisions of any other kinks with 2 or 3 for $\tau_2 < \tau < 0$, and we use similar manipulations to compute v_3. Likewise we require that kinks 3 and 4 will collide at some time in the future (with the usual restriction against collisions with other kinks) and obtain v_4 — and so forth, with alternating past and future collisions, until we reach kink $N-1$. The result of all these computations can be summarized by the relations

$$v_{i+1} = v_i - 2\frac{\Delta h_i \cdot v_i}{(\Delta h_i)^2}\Delta h_i \tag{3.28}$$

and

$$(-1)^{i+1} h_{i+1} \cdot v_i > 0 \qquad (-1)^{i+1} \vec{v}_i \cdot \left(\frac{\vec{h}_{i+1}}{h_{i+1}^{-1}} - \frac{\vec{h}_i}{h_i^{-1}} \right) > 0\,, \tag{3.29}$$

all for $1 \le i < N-1$. For fixed i, the two inequalities in eq. (3.29) are equivalent.

The only kink velocity yet to be specified is v_N. We start as before with the requirement that kinks N and 1 must have collided at some time τ_N in the past without having collided with other kinks in the time interval $\tau_N < \tau < 0$:

$$h_N + \xi_N v_N = h_1 + \zeta_1 v_1 \qquad v_N \cdot v_N = h_N \cdot v_N = 0\,, \tag{3.30}$$

with $\xi_N = \zeta_1 < 0$. We immediately obtain

$$v_N = v_1 + 2\frac{\Delta h_N \cdot v_1}{(\Delta h_N)^2}\Delta h_N \tag{3.31}$$

and the equivalent constraints

$$h_N \cdot v_1 < 0 \qquad \vec{v}_1 \cdot \left(\frac{\vec{h}_N}{h_N^{-1}} - \frac{\vec{h}_1}{h_1^{-1}} \right) < 0\,, \tag{3.32}$$

JHEP11(2015)110

where we have defined

$$\Delta h_N = h_1 - h_N\,. \tag{3.33}$$

The utility of working on a time-slice such that $h_{N-1} = h_N$ is that the equation

$$h_{N-1} + \xi_{N-1} v_{N-1} = h_N + \zeta_N v_N \tag{3.34}$$

imposes no further conditions on the v_i: this is because $\xi_{N-1} = \zeta_N = 0$. If instead we required all adjacent h_i to be distinct (including h_N and h_1), then we would have to require eq. (3.28) and eq. (3.29) for $i = 1, 2, \ldots, N$, understanding that $i = N+1$ is identified with $i = 1$. The trouble with this is that the requirement that v_{N+1} as computed from iterating eq. (3.28) once around the string should match v_1 becomes a consistency constraint on $h_1, h_2, \ldots, h_N$ together with v_1 which is difficult to solve explicitly, at least for general N. By way of contrast, our approach allows us to freely specify $\vec{h}_1, \vec{h}_2, \ldots, \vec{h}_{N-1}$, and $\vec{v}_1$ and then calculate the remaining $\vec{v}_i$ using the equations eq. (3.28) and eq. (3.31), which are linear in the $\vec{v}_i$.[3]

However, the choice of $\vec{v}_1$ is not really free: we have the inequalities eq. (3.29) and eq. (3.32), and since all the $\vec{v}_i$ are linear functions of $\vec{v}_1$, these inequalities can be cast in the form $\vec{b}_i \cdot \vec{v}_1 > 0$ for some collection of $N-1$ vectors $\vec{b}_i$, where $i = 1, 2, \ldots, N-2, N$ according to the value of i in the original inequality from which $\vec{b}_i$ arose. Each of these inequalities restricts $\vec{v}_1$ to a different half-plane in $\mathbf{R}^2$, so the combination of all of them restricts $\vec{v}_1$ to a wedge bounded by rays starting at the origin. Depending on the choice of $\vec{h}_1, \vec{h}_2, \ldots, \vec{h}_{N-1}$, this wedge may be non-empty, empty, or in a non-generic case, composed of only a single ray starting at the origin. Excluding this non-generic case from consideration, we see that the parameter space of initial conditions that we have developed is indeed $2N$-dimensional.

With the construction just described, kinks with odd i are right-moving, while kinks with even i are left-moving. This applies to kinks $N-1$ and N provided we think of them as describing the state just before their collision at $\tau = 0$. Intuitively, the orientations are as we described because, for example, kink 1 starts off to the left of kink 2 and then collides with it — so 1 must be right-moving while 2 is left-moving. To complete the construction of initial conditions, we should make sure that we can construct bases B_i for each kink with the appropriate orientation. Just before the collision of kinks 1 and 2, we may use the formulas eq. (3.19) to extract k_1 and j_2. Because neither 1 nor 2 experiences any collisions for $0 < \tau < \tau_1$, k_1 and j_2 remain unchanged over this interval, and may therefore be used at $\tau = 0$. Eq. (3.19) also tells us u_1 and w_2 at $\tau = \tau_1$, and these values may be propagated backward using a formula similar to eq. (3.13) to $\tau = 0$. The question of orientations can be settled immediately: given the expressions for k_1 and j_2 in eq. (3.19), it is immediate that eq. (3.7) holds for kink 1 as written, and eq. (3.12) holds for kink 2 without the explicit minus sign. We may then proceed to the collision between kinks 2 and 3 at time $\tau_2 < 0$ and use eq. (3.18) with $1 \to 2$ and $2 \to 3$ to deduce k_2 and j_3 (we have dropped tildes since it is understood that we are interested in basis vectors just after the collision). Eq. (3.17)

[3] In light of the non-linear relation eq. (3.22) between v_i and $\vec{v}_i$, one may question whether eq. (3.28) and eq. (3.31) really are linear in the $\vec{v}_i$. The answer is that they are, because the zero component of v_i doesn't participate in eq. (3.28) and eq. (3.31).

with $1 \to 2$ and $2 \to 3$ (and dropping tildes as before) enables us to compute u_2 and w_3. Orientation is straightforwardly verified starting with eq. (3.18). The construction of the remaining B_i proceeds similarly, with the collision of $N-1$ and N being simplest of all since one uses eq. (3.19) directly at $\tau = 0$ without having to perform any subsequent evolution of u_{N-1} or w_N.

It is worth noting that the alternating orientations we set up in the initial conditions do not generically persist as the string evolves forward in time. Indeed, the orientations of kinks $N-3, N-2, N-1, N, 1, 2$ go from perfect alternation (right-left-right-left-right-left) for τ small and negative to a different pattern (right-left-left-right-right-left) for τ small and positive, with perfect alternation elsewhere along the string for small enough τ.

4 Energy considerations

As a test of our analysis, we should be able to check that the total energy of a segmented string is conserved over time. To this end we first consider the action

$$S = -\frac{1}{4\pi\alpha'} \int_M d^2\sigma \sqrt{-h} h^{ab} \partial_a X^\mu \partial_b X^\nu G_{\mu\nu} \tag{4.1}$$

and formulate the worldsheet currents of spacetime energy-momentum:

$$P^a_\mu = -\frac{1}{2\pi\alpha'} \sqrt{-h} h^{ab} G_{\mu\nu} \partial_b X^\nu \tag{4.2}$$

Then the equation of motion following from eq. (4.1) is

$$\partial_a P^a_\mu - \Gamma^\kappa_{\mu\lambda} \partial_a X^\lambda P^a_\kappa = 0\,, \tag{4.3}$$

and if ζ_μ is a forward-directed, timelike Killing vector, we can define

$$E_\zeta = -\int d\sigma\, \zeta^\mu P^\tau_\mu\,, \tag{4.4}$$

which is constant, in the sense $\partial_\tau E_\zeta = 0$ when the equations of motion are obeyed. (We can be more general: for example, if ζ_μ is spacelike, then E_ζ would be a conserved momentum. Making ζ_μ forward-directed and timelike is the case we are interested in currently because we want E_ζ to be a measure of energy which is positive when τ increases as one moves forward in spacetime time.)

4.1 Energy of strings in AdS_3

In AdS_3, we can choose $\zeta = \partial_\tau$, and also we identify the worldsheet coordinate τ with the AdS_3 coordinate τ. Then we arrive at the definition of energy we will use:

$$E = -\int d\sigma\, P^\tau_\tau\,. \tag{4.5}$$

Next we want to evaluate the integral eq. (4.5) on a segment of string across an AdS_2 at a fixed time τ.

JHEP11(2015)110

As we have seen, an AdS_2 face is specified by a vector k with $k \cdot k = 1$. Suppose we write

$$\begin{pmatrix} k^{-1} \\ k^0 \\ k^1 \\ k^2 \end{pmatrix} = \begin{pmatrix} \sinh\kappa\cos\mu \\ \sinh\kappa\sin\mu \\ \cosh\kappa\cos\theta \\ \cosh\kappa\sin\theta \end{pmatrix} . \tag{4.6}$$

Then, using eq. (3.2), the AdS_2 face is all points Y such that

$$k \cdot Y = -\cosh\rho\sinh\kappa\cos(\mu-\tau) + \sinh\rho\cosh\kappa\cos(\theta-\phi) = 0\,. \tag{4.7}$$

Let us first treat the generic case where neither term in the middle expression in eq. (4.7) vanishes separately. Then we may solve for ρ in terms of ϕ:

$$\rho = \operatorname{arccoth}\left(\frac{\cos(\theta-\phi)}{\cos(\mu-\tau)}\coth\kappa\right) . \tag{4.8}$$

Note that the right hand side is a one-to-one function of ϕ when the image is required to be real. As a result, ϕ is a good coordinate on the worldsheet segment under consideration. One can show that

$$P^\tau_\tau = \frac{1}{2\pi\alpha'}\frac{\cos(\mu-\tau)\sinh\kappa\cos(\theta-\phi)\left[1-\cos^2(\mu-\tau)\tanh^2\kappa\right]}{\left[\cos^2(\theta-\phi)-\cos^2(\mu-\tau)\tanh^2\kappa\right]^{3/2}}\,, \tag{4.9}$$

and one must choose the sign on the square root in the denominator to make P^τ_τ positive. The energy integral between two points h_1 and h_2 (both on the same timeslice as before) is

$$E_{12} = \left|\int_{\phi_1}^{\phi_2} d\phi\, P^\tau_\tau\right| . \tag{4.10}$$

This integral can be done explicitly in terms of elementary functions, but we do not have a sufficiently simplified expression for the answer to make it useful to record explicitly here.

If both terms in the middle expression in eq. (4.7) vanish separately, then the treatment becomes a bit more subtle. In general, ρ will be non-constant along the segment we are interested in, and therefore we must have $\cos(\theta-\phi) = 0$. This means that ϕ is constant, at least on the spatial slice where we are trying to evaluate the energy. Therefore, ϕ is not a good worldsheet coordinate. It turns out that the best choice of coordinates comes from first rotating space so that $\theta = \pi/2$, so that the string runs along the $\phi = 0$ direction, and then introducing new coordinates

$$X^\mu = (\tau, Y^1, Y^2)\,, \tag{4.11}$$

where in terms of old coordinates, $(Y^1, Y^2) = (\cosh\rho\cos\phi, \cosh\rho\sin\phi)$. As usual we identify worldsheet τ with the AdS_3 coordinate τ. Because the string runs along the $\phi = 0$ direction on the timeslice of interest, we can parametrize the spatial direction of the string

JHEP11(2015)110

with Y^1. In short, $\sigma^a = (\tau, Y^1)$. Noting that $k^A = (\sinh\kappa\cos\mu, \sinh\kappa\sin\mu, 0, \cosh\kappa)$ in the new coordinate system, we find

$$P^\tau_\tau = \frac{1}{2\pi\alpha'} \frac{1-(Y^1)^2\cos^2(\mu-\tau)\tanh^2\kappa}{\sqrt{1-\frac{1}{2}\left[1+(Y^1)^2-(1-(Y^1)^2)\cos(2(\mu-\tau))\right]\tanh^2\kappa}}\,, \tag{4.12}$$

where the square root is chosen to make P^τ_τ positive. The energy may be evaluated as

$$E_{12} = \left| \int_{h^1_1}^{h^1_2} dY^1\, P^\tau_\tau \right| \,, \tag{4.13}$$

where it is understood that h^1_1 and h^1_2 are the Y^1 components of the endpoints of the string segment on the timeslice of interest. The indefinite integral of P^τ_τ with respect to Y^1 can be performed, but again its explicit form is unenlightening.

The total energy of a closed string made out of N segments is

$$E_{\text{tot}} = \sum_{i=1}^{N} E_{i,i+1}\,, \tag{4.14}$$

where we identify $N+1$ with 1. The way we have organized our presentation here, it is not transparent that E_{tot} must be constant; but conservation still follows by a general integration by parts argument on the worldsheet as a whole.

4.2 An example in AdS_3

Let's consider an example where there are $N = 4$ vertices in AdS_3. Let the initial configuration at $\tau = 0$ be a perfect square with corners at $\phi = \pi/2$, π, $3\pi/2$, and 0, corresponding to $i = 1$, 2, 3, and 4, all at the same value $\rho = \rho_0$. Thus

$$h_j = \begin{pmatrix} \cosh\rho_0 \\ 0 \\ \sinh\rho_0 \cos\frac{j\pi}{2} \\ \sinh\rho_0\sin\frac{j\pi}{2} \end{pmatrix} . \tag{4.15}$$

Let the initial velocities be

$$v_j = \begin{pmatrix} 0 \\ 1 \\ -(-1)^j \sin\frac{j\pi}{2} \\ (-1)^j\cos\frac{j\pi}{2} \end{pmatrix} . \tag{4.16}$$

The first collision after time $\tau = 0$ occurs at a time $\tau = \Delta\tau/2$ where

$$\Delta\tau = 2\arctan\tanh\rho_0\,. \tag{4.17}$$

At this time, one can easily see that

$$h_1 = h_4 = \begin{pmatrix} \cosh\rho_0 \\ \sinh\rho_0 \\ \sinh\rho_0 \\ \sinh\rho_0 \end{pmatrix} \qquad h_2 = h_3 = \begin{pmatrix} \cosh\rho_0 \\ \sinh\rho_0 \\ -\sinh\rho_0 \\ -\sinh\rho_0 \end{pmatrix} . \tag{4.18}$$

One can check that after an additional interval of time $\Delta\tau/2$, the string is again in the form of a perfect square, and after another such interval there is another double collision, with the string orthogonal to its configuration as indicated in eq. (4.18).

Now consider the energy of this string at $\tau = 0$. Because of symmetry, we can look at only one side of the square and then multiply the result by 4. To proceed with the segment between kink 4 and kink 1, we first need to observe that the vector k that defines the AdS_2 face along which this segment runs is

$$k = \begin{pmatrix} \sinh\rho_0 \\ \cosh\rho_0 \\ \cosh\rho_0 \\ \cosh\rho_0 \end{pmatrix} , \tag{4.19}$$

from which we immediately extract

$$\theta = \frac{\pi}{4} \qquad \kappa = \operatorname{arcsinh}(\sqrt{2}\cosh\rho_0) \qquad \mu = \arctan\coth\rho_0 \,. \tag{4.20}$$

Starting from eqs. (4.9)–(4.10), one can show that the total energy is

$$E_{\text{tot}} = 4E_{41} = \frac{4\sinh 2\rho_0}{2\pi\alpha'} \,. \tag{4.21}$$

As a spot-check of our calculations in the previous section, one can re-evaluate the energy at time $\tau = -\Delta\tau/2$. This is a convenient time to choose because the string spans its widest extent on the AdS_2 face described by eq. (4.19). After rotating coordinates as described above eq. (4.11), the extent of the string is from $Y^1 = -\sqrt{2}\sinh\rho_0$ to $Y^1 = \sqrt{2}\sinh\rho_0$. Applying eqs. (4.12)–(4.13) with $\tau = -\Delta\tau/2$, one swiftly arrives at

$$E_{\text{tot}} = 2E_{41} = \frac{4\sinh 2\rho_0}{2\pi\alpha'} \,, \tag{4.22}$$

where the first equality follows from noting that at time $\tau = -\Delta\tau/2$, the string runs from h_0 to h_1 and then doubles back on itself to run back from $h_2 = h_1$ to $h_3 = h_4$. The agreement between the final expressions in eq. (4.21) and eq. (4.22) is a consequence of energy conservation and serves as the desired spot-check.

4.3 Semi-classical analysis of yo-yo strings in AdS_5

In [3], long folded strings were considered which spin rigidly in global AdS_5, and which are argued to be dual to operators in $\mathcal{N} = 4$ super-Yang-Mills theory involving many

JHEP11(2015)110

gauge-covariant derivatives, such as $\operatorname{tr} X^I \nabla_{(\mu_1} \cdots \nabla_{\mu_S)} X^I$. Here $(\cdots)$ indicates traceless symmetrization so as to obtain a spin-S representation. The main calculation focuses on a string state whose dual operator is more precisely described as $\operatorname{tr} X^I \nabla_z^S X^I$ where $\nabla_z = \nabla_2 - i\nabla_3$, and ∇_2 and ∇_3 are understood as covariant derivatives in two chosen spatial directions. The energy E of the string state in global AdS_5 (rendered dimensionless by a factor of the AdS_5 radius L) is interpreted as the dimension of the dual operator, while the angular momentum of the string state is just S. An interesting expression for the twist,

$$\Delta - S = \frac{\sqrt{\lambda}}{\pi} \log \frac{S}{\sqrt{\lambda}} + \mathcal{O}(S^0)\,, \tag{4.23}$$

was recognized as relating to the cusp anomalous dimension of Wilson loops. A significant fraction of the integrability literature has been devoted to expanded understanding of this type of string / operator mapping, together with the field theory analysis of the field theory operators. In this section, we would like to pursue the semi-classical quantization of the yo-yo string in order to probe its possible relation to operators similar to the ones that describe the folded spinning string. For a related calculation based on a different classical string motion, see [19].

So far we have considered the yo-yo string in AdS_3, but the generalization to any dimension of anti-de Sitter space is obvious; in AdS of any dimension, the string worldsheet still stays within an AdS_2 subspace. We will focus on AdS_5. Following the presentation of [16], we write an action

$$S = -\frac{1}{4\pi\alpha'} \int_M d^2\sigma \sqrt{-h} h^{ab} \partial_a X^\mu \partial_b X^\nu G_{\mu\nu} + \int_{\partial M} d\xi \, \frac{1}{2\eta} \dot{X}^\mu \dot{X}^\nu G_{\mu\nu}\,, \tag{4.24}$$

where the second term is included to describe momentum at the endpoints, since in this section we are considering a single AdS_5 yo-yo. Here h_{ab} is the worldsheet metric, determined up to a conformal factor by its equation of motion, and $\eta = \eta(\xi)$ is the einbein on the boundary, whose choice is equivalent to choosing a particular coordinate ξ to parametrize the boundary. We will consider motions in global AdS_5, described as

$$ds^2 = L^2(-\cosh^2\rho\, dt^2 + d\rho^2 + \sinh^2\rho\, d\Omega_3^2)\,, \tag{4.25}$$

where $d\Omega_3^2$ is the metric on a unit S^3. For simplicity, let us set the AdS_5 radius $L = 1$.

To treat the folded string efficiently, we use t and ρ to parametrize the worldsheet; only ρ runs from 0 to ∞, such that this parametrizes only half of the worldsheet of the yo-yo centered around the origin. We thus integrate over only half the worldsheet, but will then double the resulting action. Also, we parametrize the boundary using $\xi = t$; its location will be denoted $\rho_*(t)$. The action can be rewritten as

$$S = \int dt\, \mathcal{L} \tag{4.26}$$

where

$$\mathcal{L} = -\frac{2}{\pi\alpha'} \int_0^{\rho_*} d\rho\, \cosh\rho + \frac{1}{\eta}(-\cosh^2\rho_* + \dot{\rho}_*^2) = -\frac{2}{\pi\alpha'} \sinh\rho_* + \frac{1}{\eta}(-\cosh^2\rho_* + \dot{\rho}_*^2)\,. \tag{4.27}$$

The coefficient $-2/\pi\alpha'$ on the first term comes from the coefficient $-1/4\pi\alpha'$ on the first term of eq. (4.24). One factor of 2 comes from plugging in the worldsheet metric for h_{ab}; another comes from the fact that the string is doubled over; and a third comes from the fact that we only parametrized the $\rho > 0$ half of the string. Likewise the $1/\eta$ coefficient comes from $1/2\eta$ in eq. (4.24), doubled because our parametrization only tracks one of the two endpoints.

We will now simplify notation by replacing ρ_* by ρ. We observe that the equation of motion for η simply enforces that the endpoint should move along a null trajectory. We now form the Hamiltonian

$$\begin{aligned} H &= p\dot{\rho} - \mathcal{L} \\ &= \frac{1}{\eta}(\dot{\rho} \mp \cosh\rho)^2 \pm \frac{2}{\eta}\dot{\rho}\cosh\rho + \frac{2}{\pi\alpha'}\sinh\rho \\ &= |p|\cosh\rho + \frac{2}{\pi\alpha'}\sinh\rho\,. \end{aligned} \tag{4.28}$$

In the last line we have used the null trajectory condition on the endpoint. Alternatively, we could form H as the integral of P^t_t plus endpoint contributions.

The WKB condition, used to describe a quarter of a full cycle of the motion in which the endpoint of the string starts at $\rho = 0$ and proceeds to its maximum value ρ_0, reads

$$\frac{\pi}{2}N = \int_0^{\rho_0} d\rho\, p(\rho) \tag{4.29}$$

where N is the excitation level and $p(\rho)$ is obtained by solving the equation $H = E$. Thus

$$\frac{\pi}{2}N = \int_0^{\rho_0} d\rho\, \operatorname{sech}\rho\left(E - \frac{2}{\pi\alpha'}\sinh\rho\right)\,. \tag{4.30}$$

We determine ρ_0 by setting $p(\rho_0) = 0$. When ρ_0 is large, we readily find

$$E - N = \frac{4}{\pi^2\alpha'}\log N + \mathcal{O}(N^0)\,. \tag{4.31}$$

The simplest explanation of the logarithmic term in eq. (4.31) is that the yo-yo strings are mapped to operators which are similar to the $\operatorname{tr} X^I\nabla_z^S X^I$ operators of [3], where $\nabla_z = \frac{1}{2}(\nabla_2 - i\nabla_3)$ and ∇_i for $i = 1, 2, 3$ are the gauge-covariant derivatives in the three spatial directions of the boundary theory. Specifically, consider the operator $\operatorname{tr} X^I\nabla_1^N X^I$. This operator does not transform in a definite representation of the rotation group, but it overlaps with representations with spin up to N and is annihilated by rotations which preserve the direction of the 1 axis. Heuristically, then, it is a good candidate to be mapped to the yo-yo string, which also is invariant under an abelian subgroup of rotations but can be understood to have a large total angular momentum. A striking aspect of eq. (4.31) is that the coefficient of $\log N$ is $4/\pi$ times the result of eq. (4.23) (using the conventions of [3], where $L^4 = \lambda\alpha'^2$), and we do not have a clear account for why this factor should be present.

5 Further examples

We now discuss four example evolutions of segmented strings. The first and easiest example is the square; then we deal with the regular hexagon and the regular octagon, followed by an example of irregular shape, namely an irregular hexagon.

We have written an algorithm in Mathematica that iterates the collisions. In particular we focus our attention on the analysis of the periodicity of the motion and on the conservation of the energy of the aforementioned systems of strings of various shapes. Anticipating our results, we find that the motion is periodic only in the case of the square. For other regular and irregular shapes taken into consideration the motion does not repeat itself periodically, at least not on the timescales we analyzed. Nevertheless, we verified that the energy is conserved in all cases, and this constitutes a nontrivial check of the correctness of the algorithm we used in the evolution of the motion.

As discussed in section 3.3, for each considered shape of an even number (N) of kinks we will need to specify $\vec{h}_1, \vec{h}_2, \ldots, \vec{h}_{N-1}$ and $\vec{v_1}$, in order to be able to fully determine the initial conditions. For the regular N-gon, this comes down to specifying the N-gon radius r, offset angle ϕ (defined as the angle the first vertex makes with the Y^1-axis), sign σ and magnitude of velocity v in the general formulas

$$h_N = \left(\sqrt{1+r^2},\, 0,\, r\cos\left((i-1)\frac{2\pi}{N}+\phi\right),\, r\sin\left((i-1)\frac{2\pi}{N}+\phi\right)\right), \tag{5.1}$$

$$v_N = \left(0,\, v,\, -\sigma(-1)^i v\sin\left((i-1)\frac{2\pi}{N}+\phi\right),\, \sigma(-1)^i v\cos\left((i-1)\frac{2\pi}{N}+\phi\right)\right) \tag{5.2}$$

with $i = 1, \ldots, N$.

In addition to snapshots of the string configurations shown below, we provide videos of the evolution of the string for all our examples online, see [20].

5.1 Square

As discussed earlier in section 4.2, the motion of the square is periodic, with a time interval $\Delta\tau$ between collisions and a conserved energy E that can both be calculated analytically. We performed a check on this by running the program for a square ($N = 4$) with initial conditions specified by choosing $r = \sqrt{2}$, $\phi = \pi/4$, $\sigma = 1$ and $v = r = \sqrt{2}$ in formulas eqs. (5.1)–(5.2). See [21] for the video of the evolution of the configuration. Due to the symmetry of the initial string configuration, two collisions of neighboring vertices always happen simultaneously. We have tracked the motion for 60 collision events, *i. e.*, for the first 120 collisions of vertex pairs. We observe that the events are equally spaced in AdS_3 time, with

$$\Delta\tau = 1.36944\,. \tag{5.3}$$

This means that each vertex undergoes collisions with a period of $\Delta\tau$. The energy is conserved at a value of $E = \frac{1}{2\pi\alpha'} \times 19.5959$. It is easy to see that these values agree with eq. (4.17) and eq. (4.21).

We will see in the next examples that the string trajectories are no longer periodic once $N > 4$, even when we deal with regular shapes.

JHEP11(2015)110

	h_1	h_2	h_3	h_4	h_5	h_6		v_1	v_2	v_3	v_4	v_5	v_6
-1	$\frac{\sqrt{7}}{2}$	$\frac{\sqrt{7}}{2}$	$\frac{\sqrt{7}}{2}$	$\frac{\sqrt{7}}{2}$	$\frac{\sqrt{7}}{2}$	$\frac{\sqrt{7}}{2}$	-1	0	0	0	0	0	0
0	0	0	0	0	0	0	0	1	1	1	1	1	1
1	$\frac{3}{4}$	0	$-\frac{3}{4}$	$-\frac{3}{4}$	0	$\frac{3}{4}$	1	$-\frac{1}{2}$	1	$-\frac{1}{2}$	$-\frac{1}{2}$	1	$-\frac{1}{2}$
2	$\frac{\sqrt{3}}{4}$	$\frac{\sqrt{3}}{2}$	$\frac{\sqrt{3}}{4}$	$-\frac{\sqrt{3}}{4}$	$-\frac{\sqrt{3}}{2}$	$-\frac{\sqrt{3}}{4}$	2	$\frac{\sqrt{3}}{2}$	0	$-\frac{\sqrt{3}}{2}$	$\frac{\sqrt{3}}{2}$	0	$-\frac{\sqrt{3}}{2}$

Table 1. Initial values of vectors h_i and v_i for the regular hexagon.

5.2 Regular hexagon

The initial h and v for the regular hexagon ($N = 6$) are shown in table 1. They follow from setting $r = \sqrt{3}/2$, $\phi = \pi/6$, $\sigma = -1$ and $v = 1$ in formulas eqs. (5.1)–(5.2).

We let the system evolve and find a more elaborate pattern for the motion of the strings. The sequence in figure 1 represents the motion from the beginning until the third set of collisions. Due to the symmetry of the initial configuration, all pairs of neighboring vertices always collide simultaneously. In other words, every set of collisions comprises three collisions of vertex pairs. A video of the evolution of the motion for the hexagon can be found in [22]. Conservation of energy is a useful check on the numerics. We find that

$$E = \frac{1}{2\pi\alpha'} \times 7.93725 \tag{5.4}$$

is indeed constant throughout the motion. The motion does not appear to be periodic, but a sort of quasi-periodicity is evident from the plot in figure 2 of the first 59 intervals $\Delta\tau_i$ between collisions against the times τ_i at which they occur. We will characterize this quasi-periodicity more precisely in section 5.5.

5.3 Regular octagon

We constructed the initial conditions for the regular octagon starting from formulas eq. (5.1) and eq. (5.2) with $N = 8$, $r = 1$, $\phi = \pi/4$, $\sigma = -1$ and $v = r = 1$ (with the resulting initial h and v shown in table 2 for completeness). The video of the motion of the regular octagon configuration can be found in [23]. Similar to the case of the regular hexagon, four vertex-pair collisions always happen simultaneously. The energy is conserved, as it must be, assuming the constant value

$$E = \frac{1}{2\pi\alpha'} \times 9.37258 \tag{5.5}$$

throughout the motion. As before, the motion is not periodic, but quasi-periodicity can be observed in the plot in figure 3 of the first 59 intervals $\Delta\tau_i$ between collisions.

5.4 Irregular hexagon

For the irregular hexagon, the spatial values of the positions h_N and velocity v_1 can be specified more arbitrarily. Table 3 shows the numbers we used as input to run the program (with finite precision in this case). The resulting irregular motion is depicted in figure 4 and shown

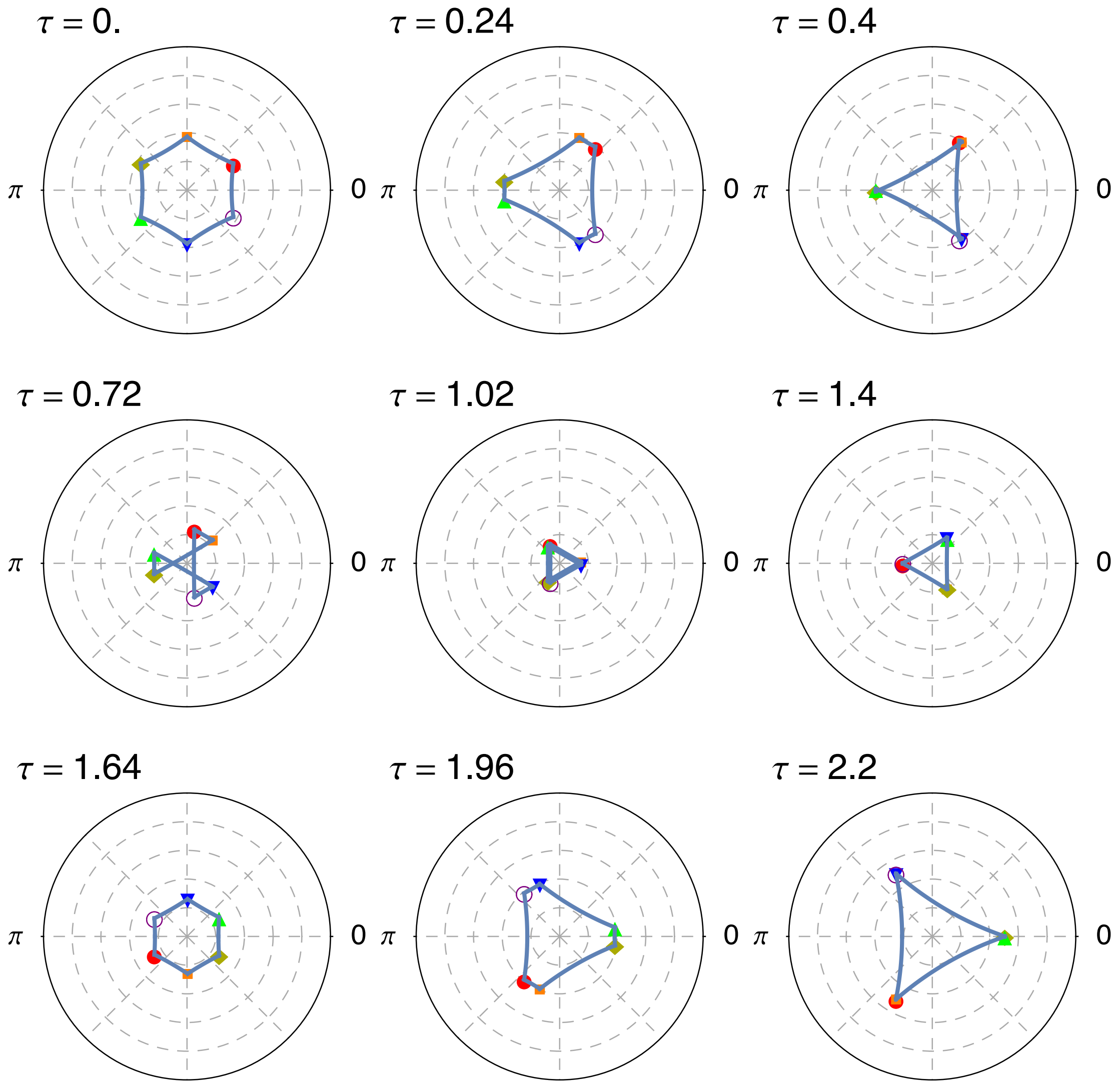

Figure 1. Pattern of motion of the regular hexagon for $0 \leq \tau \leq 2.2$. The string configuration is projected onto the Poincaré disk. Due to the regularity of the initial conditions, all vertex-pair collisions always happen simultaneously. The plots in the right column show the first nine ($= 3 \times 3$) collisions.

in the video [24]. As in the other examples considered, the irregular hexagon passes the non-trivial check that energy is conserved during the evolution of the vertices, at a value of

$$E = \frac{1}{2\pi\alpha'} \times 8.56488. \tag{5.6}$$

The pattern of collision time intervals, shown in figure 5, is irregular, as expected. No periodic structure can be distinguished.

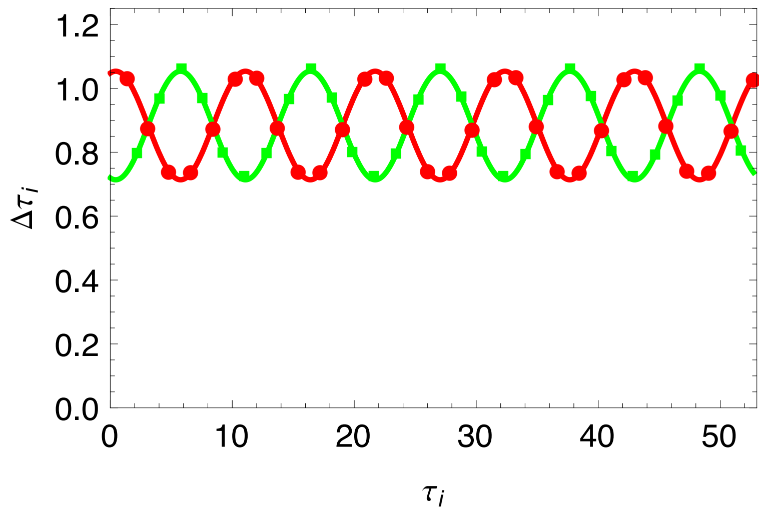

(a) Collision time intervals $\Delta\tau_i$ in AdS units, plotted versus the time τ_i at the upper end of the respective interval. At every data point three collisions happen simultaneously. The solid lines are fits of the form $a + b\sin(\omega\tau_i + \phi)$.

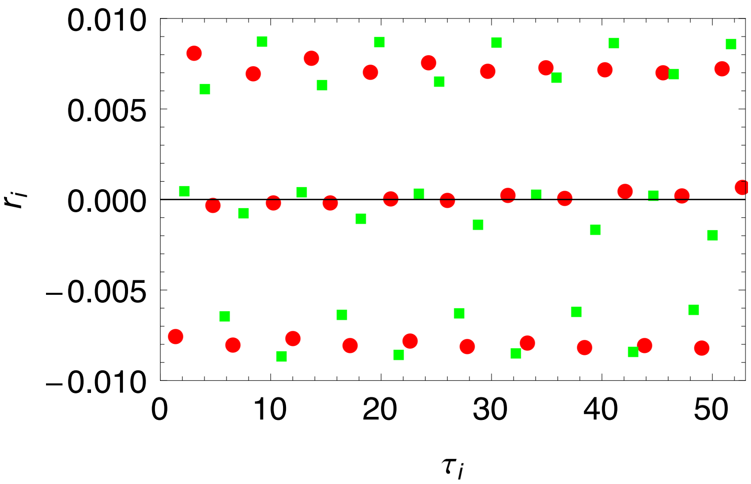

(b) Residues of the fit shown in the upper panel, plotted versus the time τ_i of collision.

Figure 2. Collision time intervals for the regular hexagon. Apparently, the data points can, alternatingly, be described by shifted sines (upper panel), with residues of order 10^{-2} (lower panel).

5.5 Patterns in the collision time intervals

For the regular N-gons with $N > 4$ that we consider, *viz.* the regular hexagon and octagon in sections 5.2 and 5.3, respectively, we found that the motion is not periodic in time. Quite intriguingly, however, the time intervals between subsequent collisions can be fitted with shifted sine functions. In the case of the hexagon, the collision time intervals $\Delta\tau_i$ appear to alternatingly follow one of two sines, cf. figure 2, whereas for the octagon there are three sines, cf. figure 3. In each of the cases, the different oscillations that we discern share the same frequency to high accuracy.

JHEP11(2015)110

	h_1	h_2	h_3	h_4	h_5	h_6	h_7	h_8
-1	$\sqrt{2}$	$\sqrt{2}$	$\sqrt{2}$	$\sqrt{2}$	$\sqrt{2}$	$\sqrt{2}$	$\sqrt{2}$	$\sqrt{2}$
0	0	0	0	0	0	0	0	0
1	$\frac{1}{\sqrt{2}}$	0	$-\frac{1}{\sqrt{2}}$	-1	$-\frac{1}{\sqrt{2}}$	0	$\frac{1}{\sqrt{2}}$	1
2	$\frac{1}{\sqrt{2}}$	1	$\frac{1}{\sqrt{2}}$	0	$-\frac{1}{\sqrt{2}}$	-1	$-\frac{1}{\sqrt{2}}$	0
	v_1	v_2	v_3	v_4	v_5	v_6	v_7	v_8
-1	0	0	0	0	0	0	0	0
0	1	1	1	1	1	1	1	1
1	$-\frac{1}{\sqrt{2}}$	1	$-\frac{1}{\sqrt{2}}$	0	$\frac{1}{\sqrt{2}}$	-1	$\frac{1}{\sqrt{2}}$	0
2	$\frac{1}{\sqrt{2}}$	0	$-\frac{1}{\sqrt{2}}$	1	$-\frac{1}{\sqrt{2}}$	0	$\frac{1}{\sqrt{2}}$	-1

Table 2. Initial values of vectors h_i and v_i for the regular octagon.

	h_1	h_2	h_3	h_4	h_5	h_6
-1	1.40046	1.40046	1.2929	1.2929	1.35095	1.35095
0	0	0	0	0	0	0
1	0.845877	0.00640535	-0.715193	-0.715193	0.0119017	0.780614
2	0.495763	0.980432	0.400119	-0.400119	-0.908246	-0.46443
	v_1	v_2	v_3	v_4	v_5	v_6
-1	0.187146	0.187146	-0.0467448	-0.0467448	0.0674737	0.0674737
0	1.16403	1.16403	0.952793	0.952793	1.0514	1.0514
1	-0.35	1.15	-0.4	-0.4	1.05	-0.45
2	1.12583	0.259808	-0.866025	0.866025	-0.0866025	-0.952628

Table 3. Initial values of vectors h_i and v_i for the irregular hexagon.

More precisely, we were able to fit the numerical data for the hexagon to the form

$$\Delta\tau_i = \begin{cases} a + b\sin(\omega\tau_i + \phi) & \text{for odd } i \\ a + b\sin(\omega\tau_i + \phi + \pi) & \text{for even } i \end{cases} \tag{5.7}$$

and the best fit parameters are

$$a = 0.883603\,, \qquad b = 0.169865\,, \qquad \omega = 0.590824\,, \qquad \phi = 1.30763\,. \tag{5.8}$$

The residuals of the fit are on order 10^{-2}, which is small but numerically significant: see the lower panel of figure 2. Sinusoidal structure can be detected in the residuals.

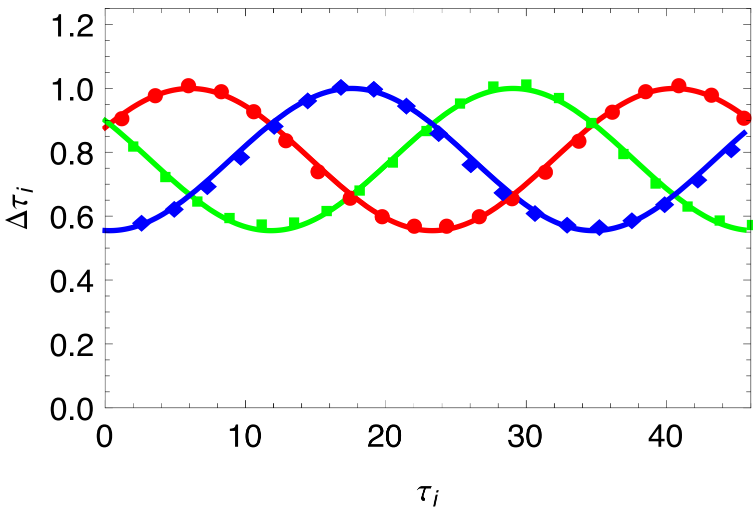

(a) Collision time intervals $\Delta\tau_i$ in AdS units, plotted versus the time τ_i at the upper end of the respective interval. At every data point four collisions happen simultaneously. The solid lines are fits of the form $a + b\sin(\omega\tau_i + \phi)$.

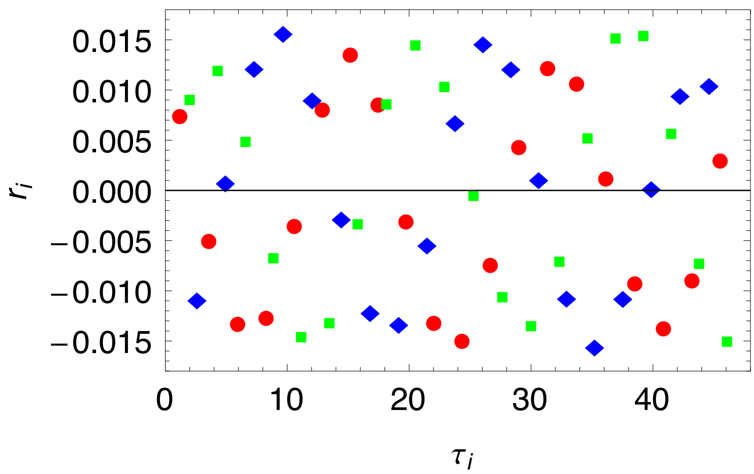

(b) Residues of the fit shown in the upper panel, plotted versus the times τ_i of collision.

Figure 3. Collision time intervals for the regular octagon. Apparently, the data points can, alternatingly, be described by shifted sines (upper panel), with residues of order 10^{-2} (lower panel).

The numerical data for the octagon can similarly be fit to the form

$$\Delta\tau_i = \begin{cases} a + b\sin(\omega\tau_i + \phi) & \text{for } i \equiv 1 \pmod 3 \\ a + b\sin(\omega\tau_i + \phi + 2\pi/3) & \text{for } i \equiv 2 \pmod 3 \\ a + b\sin(\omega\tau_i + \phi + 4\pi/3) & \text{for } i \equiv 0 \pmod 3 \end{cases} \tag{5.9}$$

and the best fit parameters are

$$a = 0.777052\,, \qquad b = 0.222491\,, \qquad \omega = 0.182199\,, \qquad \phi = 0.466574 \tag{5.10}$$

with slightly larger residuals than in the case of the hexagon. As before, sinusoidal behavior can be detected in the residuals: see the lower panel of figure 3.

JHEP11(2015)110

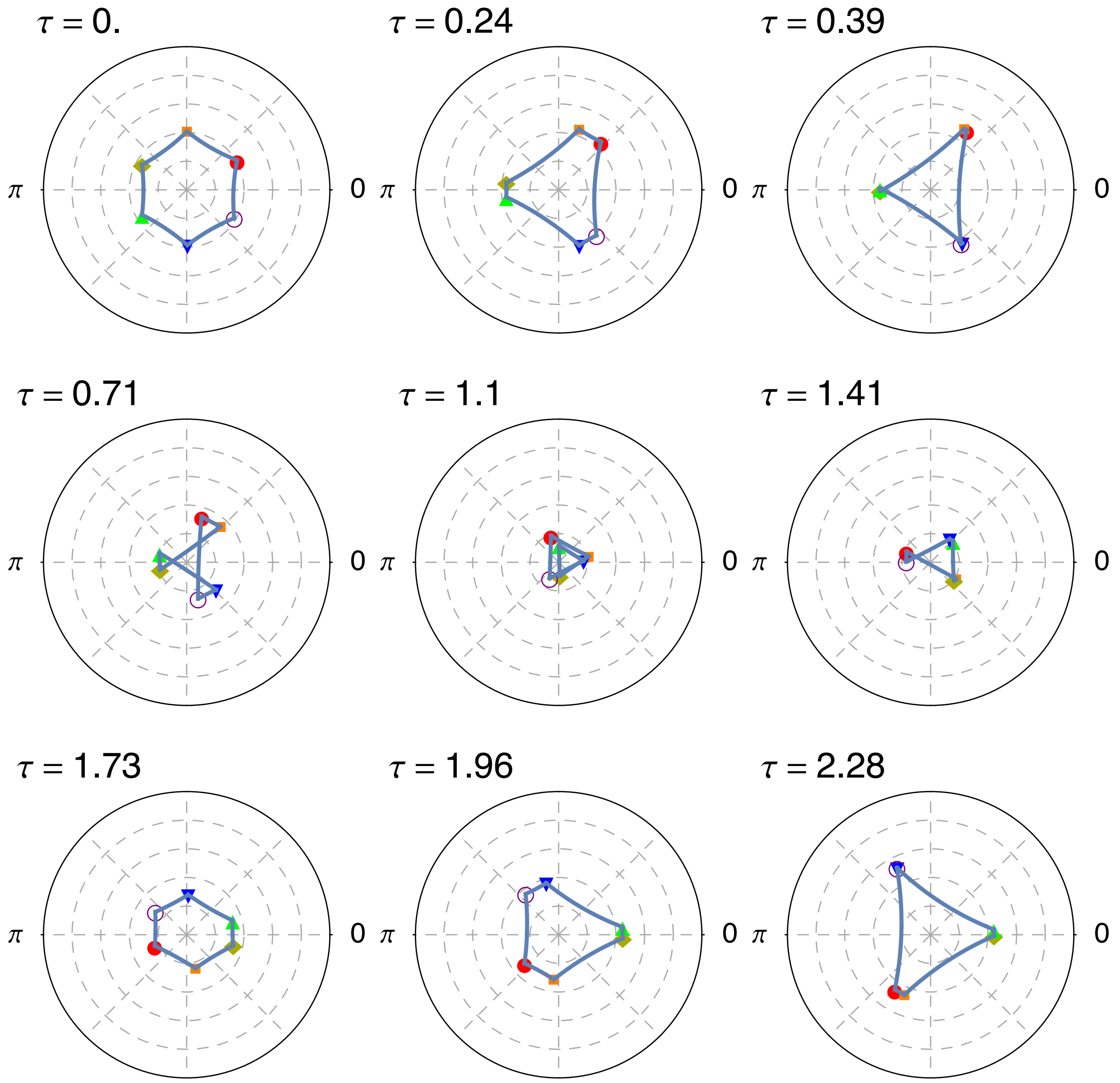

Figure 4. Pattern of motion for the irregular hexagon for $0 \leq \tau \leq 2.28$. The string configuration is projected onto the Poincaré disk. As opposed to the case of the regular hexagon and octagon, collisions of vertex pairs do not happen at the same time. The plots show the string motion up to the eighth collision.

6 Conclusions

We have explained segmented string solutions in flat space and in AdS_3, where in a given time snapshot each segment is in the flat space case a straight line, or in the AdS_3 case the intersection of an AdS_2 subspace and a surface of fixed global time. Tracking the motion of these segments is easy until their endpoints collide. As we have argued, the outcome of such collisions is in fact straightforward to predict based on considerations that can be phrased entirely locally, in terms of information arbitrarily close to the collision. The result is a pleasingly sparse specification of classical string motions, which however are exact solutions of the string equations of motion.

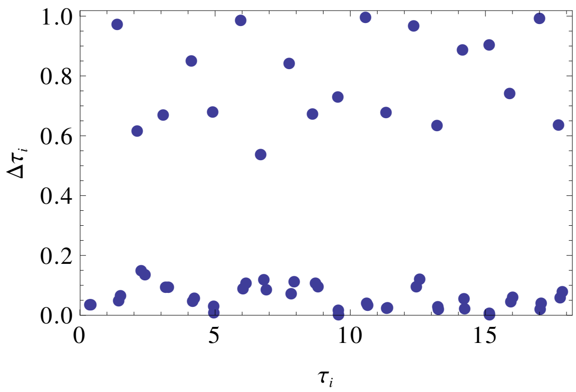

Figure 5. Collision time intervals $\Delta\tau_i$ in AdS units for the irregular hexagon, plotted versus the time τ_i at the upper end of the respective interval.

In flat space, all classical string motions with finite energy are periodic up to an overall motion of the center of mass, and of course segmented strings inherit this property. In AdS_3, the simplest segmented motions are periodic, but less simple ones are not, at least as far as we can tell. Instead we have numerical hints of a notion of quasi-periodicity, in which the time between vertex collisions cycles among several periodic functions, with small residuals which may themselves have similar representations. It seems likely that some aspect of integrability is at work, and it would clearly be appealing to find a representation of these segmented motions that makes their almost-quasi-periodic behavior manifest.

It is obvious in flat space that segmented strings can be used to approximate an arbitrary string trajectory to any desired accuracy. The simplest argument to this effect is the one following eq. (2.1), namely that arbitrary Y_R and Y_L with null tangents can be approximated by piecewise linear Y_R and Y_L where each piece is null. We have not shown that an analogous statement holds in AdS_3, but it seems to us likely that it does. Is there something fundamental about approximating a classical string by a collection of yo-yo solutions bound together at their endpoints? Is some quantum mechanical treatment available based on such a picture? A first step toward answering the second question might be to make a more systematic study of quantum states of the yo-yo, beyond the semi-classical regime, or in some improved version of the WKB treatment that we gave.

For simplicity, we have avoided localized momentum at the kinks where segments join together. This seems unnatural from the point of view of the previous paragraph, where we do our best to take seriously the assemblage of yo-yo solutions as a guide to the actual dynamics of strings. We believe that localized momentum could be included in our formalism, though obviously it would complicate the treatment of kink collisions. However, from a certain point of view it should be unnecessary. Localized momentum at a kink can be approximated by replacing the kink by two kinks very close to one another with a string segment between them that moves nearly at the speed of light. This claim can be demonstrated easily for specific motions. For example, a string that is doubled over on itself to form a closed string version of the yo-yo can be converted into a very thin rectangle. A more general demonstration would be desirable.

Localized momentum presents an interesting conceptual puzzle. What happens if we start with a very long straight string, in flat space or anti-de Sitter space, and let it collapse inward? The localized momentum at each endpoint accumulates until it back-reacts significantly on the metric, producing some version of an Aichelburg-Sexl metric, with a string coming out one side. When these shock waves collide, a black hole is formed. What comes next in the evolution? In the classical gravity picture, all that is left is a horizon, which presumably settles down to a spherical shape after some non-linear ringing. Do the early stages of the ringing approximately follow the perturbative motion of a string re-emerging from the collision with finite momentum at its endpoints? Or is the perturbative picture essentially lost because of the strong gravitational interactions?

Note added. While this paper was in preparation, we received [25], which has some overlap with the present work.

Acknowledgments

The work of N.C. was supported by a Fellowship of the Belgian American Educational Foundation. The work of S.S.G. was supported in part by the Department of Energy under Grant No. DE-FG02-91ER40671. A.S. acknowledges support in the framework of the cooperation contract between the GSI Helmholtzzentrum für Schwerionenforschung and Heidelberg University. A.S. thanks the Princeton Physics Department for hospitality. The work of A.S. at Princeton University was supported by the HGS-HIRe Abroad program and the ExtreMe Matter Institute EMMI. C.T. acknowledges support from Columbia University and from DOE grant DE-SC0011941, and thanks the Princeton Physics Department for hospitality.

References

[1] N. Beisert et al., *Review of AdS/CFT integrability: an overview*, Lett. Math. Phys. **99** (2012) 3 [arXiv:1012.3982] [INSPIRE].

[2] A.A. Tseytlin, *Review of AdS/CFT integrability, chapter II.1: classical $AdS_5 \times S^5$ string solutions*, Lett. Math. Phys. **99** (2012) 103 [arXiv:1012.3986] [INSPIRE].

[3] S.S. Gubser, I.R. Klebanov and A.M. Polyakov, *A semiclassical limit of the gauge/string correspondence*, Nucl. Phys. **B 636** (2002) 99 [hep-th/0204051] [INSPIRE].

[4] G. Arutyunov and M. Staudacher, *Matching higher conserved charges for strings and spins*, JHEP **03** (2004) 004 [hep-th/0310182] [INSPIRE].

[5] M. Kruczenski, *Spiky strings and single trace operators in gauge theories*, JHEP **08** (2005) 014 [hep-th/0410226] [INSPIRE].

[6] V.A. Kazakov and K. Zarembo, *Classical/quantum integrability in non-compact sector of AdS/CFT*, JHEP **10** (2004) 060 [hep-th/0410105] [INSPIRE].

[7] C. Kalousios, M. Spradlin and A. Volovich, *Dressing the giant magnon II*, *JHEP* **03** (2007) 020 [hep-th/0611033] [INSPIRE].

[8] L.F. Alday and J.M. Maldacena, *Gluon scattering amplitudes at strong coupling*, *JHEP* **06** (2007) 064 [arXiv:0705.0303] [INSPIRE].

[9] M. Grigoriev and A.A. Tseytlin, *Pohlmeyer reduction of $AdS_5 \times S^5$ superstring σ-model*, *Nucl. Phys.* **B 800** (2008) 450 [arXiv:0711.0155] [INSPIRE].

[10] A. Mikhailov and S. Schäfer-Nameki, *Sine-Gordon-like action for the superstring in $AdS_5 \times S^5$*, *JHEP* **05** (2008) 075 [arXiv:0711.0195] [INSPIRE].

[11] A. Jevicki, K. Jin, C. Kalousios and A. Volovich, *Generating AdS string solutions*, *JHEP* **03** (2008) 032 [arXiv:0712.1193] [INSPIRE].

[12] L.F. Alday and J. Maldacena, *Null polygonal Wilson loops and minimal surfaces in anti-de-Sitter space*, *JHEP* **11** (2009) 082 [arXiv:0904.0663] [INSPIRE].

[13] L.F. Alday, J. Maldacena, A. Sever and P. Vieira, *Y-system for scattering amplitudes*, *J. Phys.* **A 43** (2010) 485401 [arXiv:1002.2459] [INSPIRE].

[14] X. Artru, *Classical string phenomenology.* 1. *How strings work*, *Phys. Rept.* **97** (1983) 147 [INSPIRE].

[15] B. Andersson, G. Gustafson, G. Ingelman and T. Sjöstrand, *Parton fragmentation and string dynamics*, *Phys. Rept.* **97** (1983) 31 [INSPIRE].

[16] A. Ficnar and S.S. Gubser, *Finite momentum at string endpoints*, *Phys. Rev.* **D 89** (2014) 026002 [arXiv:1306.6648] [INSPIRE].

[17] I.R. Klebanov, J.M. Maldacena and C.B. Thorn, III, *Dynamics of flux tubes in large-N gauge theories*, *JHEP* **04** (2006) 024 [hep-th/0602255] [INSPIRE].

[18] T. McLoughlin and X. Wu, *Kinky strings in $AdS_5 \times S^5$*, *JHEP* **08** (2006) 063 [hep-th/0604193] [INSPIRE].

[19] J.A. Minahan, *Circular semiclassical string solutions on $AdS_5 \times S^5$*, *Nucl. Phys.* **B 648** (2003) 203 [hep-th/0209047] [INSPIRE].

[20] *Segmented strings in AdS_3 webpage*, http://www.thphys.uni-heidelberg.de/segmented-AdS-strings.

[21] *Regular square*, http://www.thphys.uni-heidelberg.de/∼holography/segmented-strings/assets/videos/reg_square/video.html.

[22] *Regular hexagon*, http://www.thphys.uni-heidelberg.de/∼holography/segmented-strings/assets/videos/reg_hex/video.html.

[23] *Regular octagon*, http://www.thphys.uni-heidelberg.de/∼holography/segmented-strings/assets/videos/reg_oct/video.html.

[24] *Irregular hexagon*, http://www.thphys.uni-heidelberg.de/∼holography/segmented-strings/assets/videos/irreg_hex/video.html.

[25] D. Vegh, *The broken string in anti-de Sitter space*, arXiv:1508.06637 [INSPIRE].

JHEP11(2015)110